Crustal structure and dynamics of the Tien Shan

L. P. Vinnik,[1] S. Roecker,[2] G. L. Kosarev,[1] S. I. Oreshin,[1] and I. Yu. Koulakov[3]

Received 22 May 2002; revised 8 August 2002; accepted 13 August 2002; published 19 November 2002.

[1] P receiver functions of many seismograph stations in the Tien Shan in central Asia show a Ps phase converted from the bottom of a fractured surficial layer with a reduction in S velocity of around 30%. In the northern Tien Shan the depth of the bottom of this layer increases sharply from a few kilometers beneath the foreland to 15 km beneath the Kyrgyz range. This low S velocity region extending to mid-crustal depths is associated with a high level of ambient seismicity and is likely caused by fluids at high pore pressure that prevent closure of cracks. The low velocity layer is absent beneath some stations in the central Tien Shan, including a region of anomalously thin crust beneath the Naryn basin. The thin crust and reduced fracturing suggest a strong lithosphere that transfers compressive stress from the Aksay plateau in the south to the Kyrgyz and associated ranges in the north. *INDEX TERMS:* 7203 Seismology: Body wave propagation; 8010 Structural Geology: Fractures and faults; 8102 Tectonophysics: Continental contractional orogenic belts. **Citation:** Vinnik, L. P., S. Roecker, G. L. Kosarev, S. I. Oreshin, and I. Y. Koulakov, Crustal structure and dynamics of the Tien Shan, *Geophys. Res. Lett.*, *29*(22), 2047, doi:10.1029/2002GL015531, 2002.

1. Introduction

[2] The Tien Shan is the world's largest and most active intracontinental orogen, but its dynamics are poorly understood. Recent GPS measurements [*Abdrakhmatov et al.*, 1996] and geologic studies [e.g., *Thompson et al.*, 2001] in the Kyrgyz Tien Shan demonstrate how deformation is occuring at the near-surface, with most of the 20 mm/yr of convergence being taken up by slip on 4–5 active faults. However, it is not clear how deformation measured at the surface relates to deformation at depth, and what factors control where and how this deformation takes place.

[3] We investigate the state of the upper crust with the P receiver function technique. A few such studies have already been conducted in the Tien Shan [*Kosarev et al.*, 1993; *Chen et al.*, 1997; *Bump and Sheehan*, 1998; *Roecker*, 2001], but our work differs from them in several respects. First, the number of digital broad-band seismographs that we use (more than 30, Figure 1) is much larger than previously. Second, our data set provides better azimuthal coverage of the remote seismicity, and in some instances this is of crucial importance. Third, our technique allows us to observe converted phases that are delayed by about 1 s or less relative to the main P wave arrival, and the analysis of these phases is the main objective of our study.

[4] Of particular interest for our study are recent estimates of crustal thickness in the Tien Shan with the S receiver function technique [*Oreshin et al.*, 2002]. The crust is about 45 km thick in the neighboring platforms and 55–65 km thick in the mountains, although it thins to about 45 km in the central Tien Shan, where the altitude is more than 1 km higher than in the platforms (Figure 1).

2. Data and Analysis

[5] We project the teleseismic record on 3 orthogonal axes: P (or L), SV (or H, or Q) and T [*Vinnik*, 1977]. Axis P corresponds to the principal motion direction of the P wave in the vertical plane containing the source and the receiver. Axis SV is perpendicular to P in the same plane and is optimal for observing the converted Ps phases. The principal motion direction is determined in a broad band, where the dominant period of the P wave is around 1–2 s. The receiver functions are obtained by deconvolving the SV and T components by the P component. The receiver functions shown here are low-pass filtered with a corner at around 5 s. While the main features in the raw and low-pass filtered receiver functions are essentially the same, the filtered functions look relatively simple and are more convenient for presentation.

[6] The seismograph stations that we use belong to 4 networks: KNET (9 stations), IRIS/GSN (TLG and AAK), Geoscope (WUS) and GHENGIS (24 stations). The stations of the first three networks have operated for about a decade. All stations are installed on crystalline/metamorphic rocks of Precambrian or Palaeozoic age except KNET station ESK2, which is located on consolidated sediments. The GHENGIS network operated for around 18 months [*Roecker*, 2001]. Stations within Kyrgyzstan and Kazakhstan were installed on crystalline/metamorphic basement rocks, while several stations in China (KASH, WQIA, TGMT, HARA, XIKR, HLQI, KOPG and PIQG) were installed on loose sediments. Sediment thicknesses beneath the Chinese stations vary from a few 100 m beneath HLQI to as much as 10 km in the vicinity of KASH.

[7] We assembled a set of P wave recordings in a distance range from 30°–110°. Occasionally we used PP phases at epicentral distances exceeding 110°. PP phases make a significant contribution to back azimuths between 320°–360°, where good recordings of P are few. The receiver functions were stacked in azimuthal bins 20° wide to suppress noise. For stations that operated for about a decade (AAK, TLG, WUS and the KNET network) the azimuthal coverage is excellent: typically more than 200 events were processed at each of these stations, and the average number of receiver functions per azimuthal bin exceeds 10. The standard error for a summary receiver function normalized

[1]Institute of Physics of the Earth, Moscow, Russia.
[2]Rensselaer Polytechnic Institute, Troy, N.Y., USA.
[3]Institute of Geology, Novosibirsk, Russia.

0094-8276/02/2002GL015531$05.00

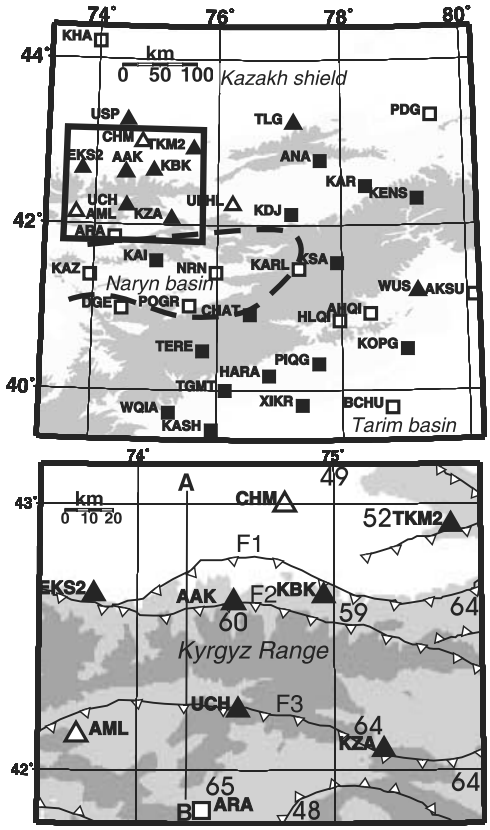

Figure 1. Maps of the region. Long-term seismograph stations and those of the GHENGIS network are shown by triangles and squares, respectively. Stations with and without the surficial low-velocity layer are shown by filled and open symbols, respectively. Altitudes higher than 1500 m and 3000 m are shown by lighter and darker shadings. The lower map is a blow-up of the rectangular region shown in the upper map. Fault notations F1, F2 and F3 are adopted from *Ghose et al.* [1998]. Dashed line in the upper map shows the region with anomalously thin crust; the numbers in the lower map indicate crustal thickness in km, after *Oreshin et al.* [2002].

to the maximum of the deconvolved P phase is around 0.02. Most of the GHENGIS network stations provide standard errors of around 0.02 for back azimuths between 60° and 160°, although the deviations at stations HARA, KOPG, KASH and BCHU can be significantly higher.

[8] In the SV components of some of the receiver functions (examples in left column of Figure 2), the first clearly visible arrival is the Ps phase from the Moho, which arrives at about 6 s after P. However, at several stations (right column of Figure 2), the first clearly visible converted phase arrives about 1 s after P. The polarity of this phase is the same as that from the Moho, which indicates that it is converted from the bottom of a low-velocity layer. The largest amplitudes are observed at stations installed on unconsolidated sediments (WQIA and TGMT in Figure 2), but, surprisingly, these phases are also present in recordings of several stations installed on hard rock (Figure 1). Amplitudes at these hard rock stations vary between approximately 0.07 and 0.15 with an average value around 0.11, which is several times larger than the standard error (around 0.02). For the remainder of this paper we focus on the origin of these unusual arrivals.

[9] The amplitude of the Ps phase depends primarily on the S velocity contrast at the discontinuity. For a sharp boundary, a converted phase amplitude of 0.11 at a representative (for our dataset) epicentral distance of 65° is produced by an S velocity contrast of 1 km/s. Amplitudes of the Ps phases from sharp and gradational boundaries are similar if the thickness of the boundary layer is not much larger than about half the S wavelength (from 3 to 10 km in our data).

[10] We can estimate the structure that produces the converted phases by adopting typical P and S velocities. The P velocity of a typical crystalline/metamorphic rock (granitic gneiss) at a depth of a few kilometers is about 6 km/s [*Christensen and Mooney*, 1995]. For a standard Poisson's ratio the corresponding S velocity is about 3.5 km/s. A 1 km/s S velocity contrast means the S velocity in the low-velocity layer should be around 2.5 km/s. A delay of 1 s thus corresponds to a layer thickness of around 5 km. The same effect could be expected if a layer with a normal velocity (3.5 km/s) were underlain by a medium with the S velocity around 4.5 km/s. This, however, is very unlikely, because the velocity of 4.5 km/s is characteristic of the mantle, and the geophysical signatures of such a large dense body at shallow depth have never been observed here.

[11] We can think of two possible explanations for the very low S velocity in the upper crustal layer beneath stations on crystalline/metamorphic rocks. First, the rocks at the surface might have overthrust sediments. This is tectonically feasible, but implies some features in the waveforms that we do not observe. If the underthrust layer were less than 5 km thick it would be transparent to waves with periods of 6 s or more. At shorter periods (or greater thicknesses), the phases converted from the top and bottom of the layer would display a complicated interference pattern that we do not observe. An alternative explanation is that the crystalline/metamorphic rocks themselves are extensively fractured and filled with fluids. Cracks and pores reduce elastic wave velocity relative to that in the uncracked solid by an amount depending on the crack density parameter ϵ [*O'Connell and Budiansky*, 1974]. For dry cracks an S velocity reduction of 30% requires an ϵ of

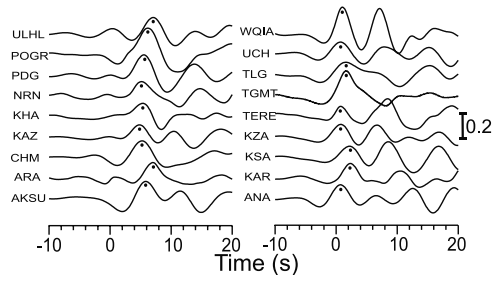

Figure 2. Examples of the SV component of the summary receiver functions in the back azimuthal sector of 100°–120°. Average epicentral distances for stations in these azimuths are between 60°–67°. Left column shows examples where the first Ps phase is from the Moho (around 6 s), while the right column shows the Ps phase from the bottom of a surficial low-velocity zone (around 1 s).

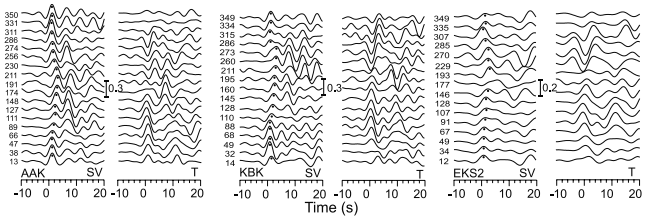

Figure 3. SV and T components of the summary receiver functions of stations AAK (left), KBK (center) and ESK2 (right). Back azimuths (in degrees) are shown on the left.

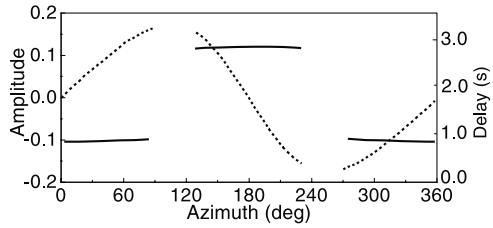

Figure 5. Travel times of the Ps phase in the SV component (solid line) and amplitude of the P phase in the T component (dash line) for the model described in the text.

about 0.3, within the range of values often found in rock samples. Pressure at a depth of a few kilometers is sufficient to close dry cracks, but fluid saturated cracks may remain open at higher pressures.

3. Kyrgyz Range

[12] Of the stations associated with the low-velocity layer, GSN/IRIS station AAK and KNET stations KBK and EKS2 are of particular interest because their data are of high quality and they reveal a similar pattern. The SV component of the Ps phase from the shallow discontinuity is clearly seen from all azimuths (Figure 3) at these stations. However, the time of this phase changes from 1 s for arrivals from the north to 3 s for those from the south, while its amplitude shows only minor variations with azimuth. The main feature in the T component is a phase at around 0 s, the amplitude of which varies azimuthally with a period of 360°. The maximum amplitudes (0.2) are observed for arrivals from the east and west. The arrival of this phase at 0 s means that it is a result of a side refraction of P, and the azimuthal dependence is consistent with a planar discontinuity dipping to the south [e.g., *Savage*, 1998].

[13] Tomographic images of P and S velocities in this region [*Ghose et al.*, 1998] show low velocities at mid-crustal depths beneath the Kyrgyz range. Qualitatively this is consistent with the larger traveltimes of the Ps phase from the south relative to those from the north. However, the 1 km/s contrast we infer from the Ps amplitude is several times larger than any variation seen in the S velocity models by *Ghose et al.* [1998]. Most of the P and S velocity cross-sections of *Ghose et al.* [1998] suggest that the crust beneath the Kyrgyz range is separated from that beneath the foreland by a discontinuity dipping to the south, which is qualitatively consistent with the wave pattern in the T component (Figure 3).

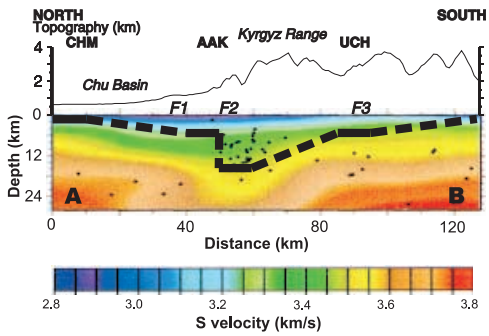

Figure 4. Cross-section of seismic structures corresponding to line AB in Figure 1. Topography of the bottom of the low-velocity zone (black line) is superimposed on the tomographic S velocity model of *Ghose et al.* [1998]. Interpolated values for the bottom of the zone are shown by a dashed line. Color bar indicates velocities in the tomographic model in km/s. Note concentration of ambient seismicity within the low-velocity zone beneath the Kyrgyz range (black dots, after *Ghose et al.* [1998]).

[14] We conducted a series of ray tracing experiments in order to find out if the wavefields in the SV components (Figure 3) can be explained by a dipping base of the low-velocity layer. For realistic P and S velocities (4.6 km/s and 2.5 km/s in the upper layer; 6.0 km/s and 3.5 km/s in the lower layer) and a dip of 10°–50°, amplitudes of the Ps phase from the north are several times smaller than those from the south, whereas the difference in the travel times is about 0.1 s. Thus, models with a dipping boundary predict amplitude variations in the SV component that are not observed, and do not predict the observed traveltime variations.

[15] The only alternative model we can propose is a flat discontinuity which changes its depth abruptly between the Kyrgyz range and the foreland (Figure 4). For the assumed P and S velocities, the depth of the discontinuity changes from 5 km beneath the foreland to 15 km beneath the Kyrgyz range. This model, however, does not explain the pattern in the T component. To explain both the SV and T components we introduce a Moho dipping to the south at 14°. The resulting traveltimes of the Ps phase in the SV component and the amplitudes of the P wave in the T component are similar to those observed (Figure 5). The gaps in the plots in the azimuths around 90° and 270° are caused by arrivals of waves reflected from the near-vertical boundary in the model; these waves don't exist in the real wavefield, as our wavelengths are comparable with the size of the wall (10 km). We note that the assumption of the dipping Moho boundary is consistent with current estimates of its depth (Figure 1). At the surface, the near-vertical boundary most closely corresponds to the fault F2 in Figure 1.

4. Discussion

[16] We have found that under several stations in the Tien Shan, the S velocity in a few uppermost kilometers is about 30% lower than in the underlying medium. Explanation of the low velocity by unconsolidated sediments is unlikely for the stations in Kyrgyzstan and Kazakhstan, and fracturing appears to be the only viable alternative. Beneath part of the Kyrgyz range the depth to the bottom of the low velocity layer abruptly changes from 5 to 15 km. Among the stations

where this sharp change is observed, one (EKS2) is installed on sediments, but the observed wave pattern is similar to that at the neighboring station AAK, which is installed in a tunnel in basement rocks. The anomalous crustal body beneath the Kyrgyz range is associated with an increased level in ambient seismicity (Figure 4), suggesting a genetic relationship between them.

[17] Open fractures can be prevented from closing at depths of 10–15 km by high fluid pressure that counters the confining lithostatic pressure [*Eberhart-Phillips et al.*, 1995]. S velocity is especially sensitive to this effect. Fluid-filled fractures decrease the electrical resistivity of rocks, and an anomaly beneath the Kyrgyz range was detected by magnetotelluric soundings in the Tien Shan [*Trapeznikov et al.*, 1997]: electrical resistivity at depths less than 25 km is 200 ohm-m, much lower than the 2000–5000 ohm-m found in neighboring regions.

[18] Evidence of velocity anomalies of comparable magnitude has been found in fault zones at depths reaching a few kilometers [e. g., *Thurber et al.*, 1997]. Published seismic data for active faults often reveal low-velocity zones not wider than a few hundred meters, but beneath the Kyrgyz range this zone should be much wider, because it is detected at frequencies at least an order of magnitude lower than those of other observations. Moreover, the coincident results at three stations separated by several tens of kilometers from each other would be practically impossible if this low-velocity zone were very narrow. Also, the related resistivity anomaly [*Trapeznikov et al.*, 1997] and the zone of ambient seismicity (Figure 4) are about 20 km wide. The results of magnetotelluric sounding suggest that similar structures may exist elsewhere in the Tien Shan, but a dense network of seismic stations that is necessary for detecting such structures is available only for the Kyrgyz range.

[19] The region to the south of the Kyrgyz range is distinguished by the absence of evidence for the surficial low-velocity layer at several stations (Figure 1). Most of these stations (ARA, KAZ, DGE, POGR, NRN, ULHL, KARL) are in a region surrounding the Naryn basin. The crust beneath several of these stations (ARA, KAZ, NRN, POGR) is anomalously thin (around 45 km) [*Krestnikov and Nersesov*, 1962; *Roecker*, 2001, *Oreshin et al.*, 2002]. A reduced crack density suggests that the crust in this region is less deformed than elsewhere. This is consistent with the anomalous crustal thickness that might be preserved from pre-orogenic time. We note that there is evidence from geology [*Abdrakhmatov et al.*, 2002] for substantial active shortening within the Naryn basin. However, this shortening appears to occur along sub-horizontal, north-dipping thrusts in sedimentary rock. These observations can be reconciled with our interpretation if the sedimentary layer is detached from the underlying metamorphic/crystalline basement, where deformation is less pronounced. This inference is corroborated by the relatively low level of ambient seismicity within the central Tien Shan.

[20] Based on these results, we suggest that the lithosphere beneath and around the Naryn basin is capable of transmitting stress from the Aksay plateau in the south to the weaker Krygyz and associated ranges in the north. Dynamically, it is analogous to the Tarim basin, which transfers stress from the Tibetan plateau to the Tien Shan. A similar correspondence was proposed for the Ferghana basin to the west by *Burov and Molnar* [1998], and may apply as well to the basin under lake Issyk-Kul. The evolution of the Tien Shan may therefore be strongly influenced by local strength heterogeneities in the lithosphere on the order of several 10's of km in lateral dimension.

[21] **Acknowledgments.** The work was supported by NSF Continental Dynamics project EAR-9614113 and by CRDF project RG2-2234. The instruments used in the collection of the GHENGIS data were provided by the IRIS PASSCAL program. Data for KNET AAK, TLG and WUS were obtained from the IRIS Data Management Center. We benefited from discussions with Peter Molnar and Ray Weldon.

References

Abdrakhmatov, K. Ye., et al., Relatively recent construction of the Tien Shan inferred from GPS measurements of present-day crustal deformation rates, *Nature*, *384*, 450–453, 1996.

Abdrakhmatov, K., R. Weldon, S. Thompson, D. Burbank, C. Rubin, M. Miller, and P. Molnar, Onset, style, and current rate of shortening in the central Tien Shan, Kyrgyz Republic, *J. Geophys. Res*, submitted to, 2002.

Bump, H. A., and A. F. Sheehan, Crustal thickness variations across the northern Tien Shan from teleseismic receiver functions, *Geophys. Res. Lett.*, *25*, 1055–1058, 1998.

Burov, E. B., and P. Molnar, Gravity anomalies over the Ferghana valley (Central Asia) and intracontinental deformation, *J. Geophys. Res.*, *103*, 18,137–18,152, 1998.

Chen, Y. H., S. W. Roecker, and G. L. Kosarev, Elevation of the 410-km discontinuity beneath the central Tien Shan; evidence for a detached lithospheric root, *Geophys. Res. Lett.*, *24*, 1531–1534, 1997.

Christensen, N. I., and W. D. Mooney, Seismic velocity structure and composition of the continental crustal: A global view, *J. Geophys. Res.*, *100*, 9761–9788, 1995.

Eberhart-Phillips, D., W. D. Stanley, B. Rodriguez, and W. J. Lutter, Surface seismic and electrical methods to detect fluids related to faulting, *J. Geophys. Res.*, *100*, 12,919–12,936, 1995.

Ghose, S., M. Hamburger, and J. Virieux, Three-dimensional velocity structure and earthquake locations beneath the northern Tien Shan of Kyrgyzstan, central Asia, *J. Geophys. Res.*, *103*, 2725–2748, 1998.

Kosarev, G. L., N. V. Petersen, L. P. Vinnik, and S. W. Roecker, Receiver functions for the Tien Shan analog broadband network: Contrasts in the evolution of the structures across the Talasso-Ferghana fault, *J. Geophys. Res.*, *98*, 4437–4448, 1993.

Krestnikov, V. N., and I. L. Nersesov, Tectonic structure of the Pamirs and Tien Shan and its relation to topography of the Moho boundary, *Soviet Geology*, *11*, 36–69, 1962.

O'Connell, R. J., and B. Budiansky, Seismic velocities in dry and saturated cracked solids, *J. Geophys. Res.*, *79*, 5412–5426, 1974.

Oreshin, S., L. Vinnik, D. Peregudov, and S. Roecker, Lithosphere and asthenosphere of the Tien Shan imaged by S receiver functions, *Geoph. Res. Lett*, 10.1029/2001GL014441, 2002.

Roecker, S., Constraints on the crust and upper mantle of the Kyrgyz Tien Shan from the preliminary analysis of GHENGIS broad-band data, *Russian Geology and Geophysics*, *42*, 1554–1565, 2001.

Savage, M. K., Lower crustal anisotropy or dipping boundaries? Effects on receiver functions and a case study in New Zealand, *J. Geoph. Res.*, *103*, 15,069–15,087, 1998.

Thompson, S. C., R. J. Weldon, C. M. Rubin, P. Molnar, K. Abdrakhmatov, and G. W. Berger, Late Quaternary slip rates across the central Tien Shan, Kyrgyz Republic, Central Asia, *J. Geophys. Res.*, in press, 2001.

Thurber, C., et al., Two-dimensional seismic image of the San Andreas fault in the northern Gabilan range, central California: Evidence for fluids in the fault zone, *Geoph. Res. Lett.*, *24*, 1591–1594, 1997.

Trapeznikov, Yu. A., E. B. Andreyev, B. Yu. Butalev, M. N. Berdichevsky, L. L. Vanian, A. M. Volikhin, N. S. Golubtsova, and A. K. Rybin, Magnetotelluric soundings in the Kyrgyz Tien Shan mountains, *Fizika Zemli*, *1*, 3–20, in Russian, 1997.

Vinnik, L. P., Detection of waves converted from P to SV in the mantle, *Phys. Earth Planet. Inter*, *15*, 39–45, 1977.

L. P. Vinnik, G. L. Kosarev, and S. I. Oreshin, Institute of Physics of the Earth, B. Grouzinskaya 10, 123995 Moscow, Russia.

S. W. Roecker, Rensselaer Polytechnic Institute, Troy, NY 12180, USA.

I. Yu. Koulakov, Institute of Geology, Koptug ave. 3, 630090 Novosibirsk, Russia.